

**NOTE:**  
***DUE TO SCANNING DEFICIENCIES, DOCUMENT IN THIS FORMAT HAS NOT BEEN  
VERIFIED BY AUTHOR***

***ORIGINALLY  
REPRINTED FROM***

***JOURNAL OF HYDROLOGY***

***JOURNAL OF HYDROLOGY 200 (1997) 323-344***

Observations of particle movement in a monitoring well using  
the colloidal borescope

Peter M. Kearl

*Environmental Sciences Division, Oak Ridge National Laboratory, Grand Junction, CO, USA 81501*  
Received 28 August 1996; revised 31 January 1997; accepted 31 January 1997

# Observations of particle movement in a monitoring well using the colloidal borescope

Peter M. Kearl

*Environmental Sciences Division, Oak Ridge National Laboratory, Grand Junction, CO, USA 81501*

Received 28 August 1996; revised 31 January 1997; accepted 31 January 1997

## ***Abstract***

The colloidal borescope consists of a set of lenses and miniature video cameras capable of observing natural particles in monitoring wells. Based on field observations of these particles, it appears possible to measure in situ groundwater velocity in a well bore. Field observations have shown that directional measurements using the colloidal borescope are generally in good agreement with expected flow directions. However, the magnitude of flow velocity is higher compared with values based on conventional test methods. High relative flow velocities, even after correction factors have been applied to compensate for well bore effects, are believed to be due to preferential flow zones in the surrounding aquifer. Low flow zones exhibit swirling multidirectional flow that does not allow for a linear velocity measurement. Consequently, groundwater flow velocities measured by the colloidal borescope in heterogeneous aquifers will be biased toward the maximum velocity values present in the aquifer. A series of laboratory experiments was conducted to assess the reliability of the instrument. Based on this work, a seepage velocity correction factor ( $d_i$ ) of 1-4 was found for quantifying groundwater seepage velocity in the adjacent aquifer from observations in a well bore. Laboratory measurements also indicate that preferential flow in the surrounding aquifer dominates flow in the well. Results of this work suggest the possibility of quantifying higher-flow velocities associated with preferential flow zones in the subsurface. (D 1997 Elsevier Science B.V.)

*Keywords:* Colloidal borescope; monitoring well; Particle movement; Flow velocity

Accurately measuring groundwater flow velocity has been a goal of researchers for a number of years, particularly with the increased emphasis on subsurface transport processes at hazardous waste sites. Conventional methods have relied on estimates of hydraulic conductivity and calculations based on Darcy's law to estimate seepage velocity in the aquifer. Methods that stress the aquifer such as bail, slug, or pumping tests have been used for years to estimate aquifer hydraulic conductivity. Recently, borehole flow meters have been used to evaluate the hydraulic conductivity of individual zones in test wells (Hess, 1986; Molz et al., 1989; Molz et al., 1994).

Directly assessing groundwater seepage velocities from flow velocities in a well is feasible based on theoretical and experimental evidence. Potential flow theory solutions describing flow through a cylinder of finite or infinite permeability surrounded by a porous medium of finite permeability have been studied by Ogilvi (1958), Carslaw and Jaeger (1959), and Wheatcraft and Winterberg (1985). Drost et al. (1968) have shown by laboratory tracer tests that groundwater flow in a porous medium with a cylinder of infinite permeability behaves as predicted by potential flow theory (Fig. 1(a) and (b)). Based on these theoretical predictions and experimental evidence, researchers have explored methods to measure flow velocities in wells in order to predict seepage velocities in the adjacent porous medium. Borehole dilution methods (Halevy et al., 1967; Drost et al., 1968; Grisak et al., 1977), the KV heat-pulsing flow meter (Kerfoot, 1988), and the laser doppler velocimeters (Momii et al., 1993) are all attempts to measure the groundwater velocity in a well.

*P.M. Kearl/Journal of Hydrology 200 (1997) 323–344*

aquifer. Methods that stress the aquifer such as bail, slug, or pumping tests have been used for years to estimate aquifer hydraulic conductivity. Recently, borehole flow meters have been used to evaluate the hydraulic conductivity of individual zones in test wells (Hess, 1986; Molz et al., 1989; Molz et al., 1994).

Directly assessing groundwater seepage velocities from flow velocities in a well is

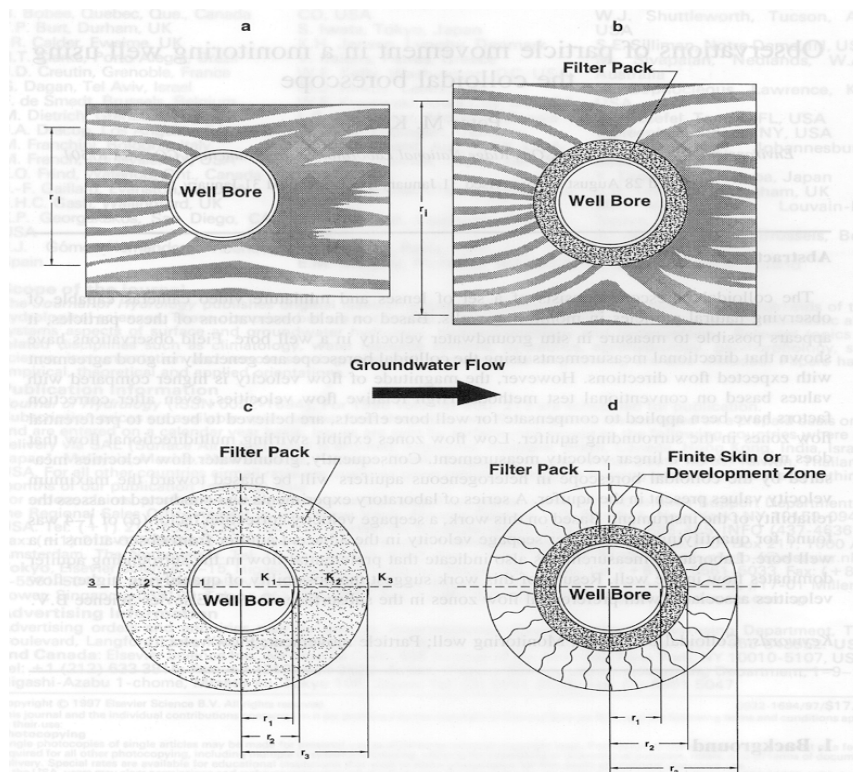


Fig. 1. Dye tracers (shaded areas) and associated well geometries for (a) flow pattern surrounding a well without a filter pack, (b) flow pattern surrounding a well with a filter pack, (c) a well surrounded by two concentric filter zones (well screen and filter pack), (d) a well surrounded by two concentric filter zones (a filter pack and a finite skin).

The colloidal borescope developed by Oak Ridge National Laboratory is another effort to measure groundwater velocity in a well. Unlike previous attempts to determine groundwater velocity in a well, the colloidal borescope provides a direct field measurement of the water velocity in a well. By directly observing naturally occurring particles that are advected by

groundwater movement, it is possible to relate flow in a well bore to the surrounding porous media.

Field observations using the colloidal borescope have been encouraging. Zones of steady horizontal laminar flow in a constant direction for several days have been observed. Directional measurements using the borescope have generally matched expected flow directions where sufficient control is present. Flow velocity measurements in the field, however, are consistently greater than predicted by conventional methods such as pumping tests used with potentiometric maps and estimates of porosity.

The purpose of this paper is to report the results of laboratory experiments designed to assess the reliability of the colloidal borescope. It is possible that preferential flow zones due to aquifer heterogeneity are responsible for the higher flow velocities observed by the colloidal borescope. However, to assess the impact of preferential flow zones on groundwater velocity measurements in the field, the influence of a well bore in a porous flow field must be assessed. If laboratory measurements of groundwater flows using the colloidal borescope agree with theoretical models, then the field velocity measurements may represent flow in preferential zones in the aquifer.

### ***Instrument description***

The colloidal borescope consists of two CCD (charged-couple device) cameras, a ball compass, an optical magnification lens, an illumination source, and stainless steel housing. The device is approximately 89 cm long and has a diameter of 44 mm, thus facilitating insertion into a 5-cm-diameter monitoring well (Fig. 2). Upon insertion into a well, an electronic image magnified 140 x is transmitted to the surface, where it is viewed and analyzed. The compass is viewed by one of the CCD cameras in order to align the borescope in the well. As particles pass beneath the lens, the back lighting source illuminates the particles similar to a conventional microscope with a lighted stage. A video frame grabber digitizes individual video frames at intervals selected by the operator. A software package developed by Oak Ridge National Laboratory compares the two

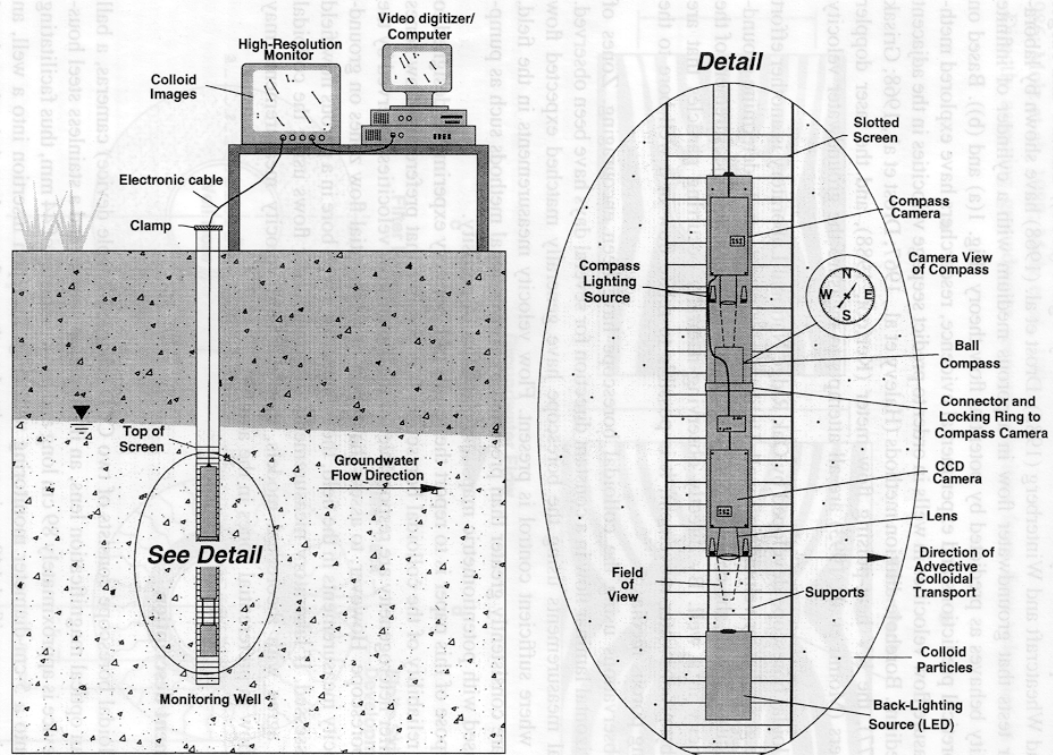


Fig. 2. Diagram of the components of the colloidal borescope. Total length of instrument is 88.9 cm, length of light source is 12.7 cm, opening between lower camera and light source is 4.3 cm, and the instrument diameter is 4.4 cm.

digitized video frames, matches particles from the two images, and assigns pixel addresses to the particles. Using this information, the software program computes and records the average particle size, number of particles, speed, and direction. A pentium based computer is capable of analyzing flow measurements every 4 s resulting in a large database after only a few minutes of observations. Since standard VHS video uses 30 frames s<sup>-1</sup>, a particle that moves 1 mm across the field of view could be captured in subsequent frames 1/30 of a second apart. This would result in an upper measurement velocity range of 3 cm s<sup>-1</sup>. For low flow conditions, the delay between frames can be set for large time periods resulting in a lower velocity range for stagnant flow conditions.

Flow velocities measured by the colloidal borescope were verified using a laminar flow chamber developed at the Desert Research Institute in Boulder City, Nevada. At a flow velocity in the laminar flow chamber of 0.10 cm s<sup>-1</sup>, and verified by a tracer test, the colloidal borescope measured a comparable velocity value of 0.11 cm s<sup>-1</sup>.

Finally, work based on borescope observations has been used to support micropurge sampling as an effective way to obtain groundwater samples representative of the total mobile pollutant load (Kearl et al., 1994).

### ***Field observations***

The colloidal borescope has been tested at several sites across the United States. Particles as small as 10  $\mu\text{m}$  can be observed. Flow velocities from stagnant conditions upward to 3-cm s<sup>-1</sup> can be measured. The number of particles often changes with time. Disturbances in ambient groundwater flow caused by the insertion of the borescope into the well result in hundreds of particles ranging in sizes from 1  $\mu\text{m}$  to over 50  $\mu\text{m}$ . After a few minutes, particle numbers and sizes generally decrease. In certain aquifers, particularly sandy permeable aquifers with low organic material or clay content, the number of visible particles may decrease to 1-2 min<sup>-1</sup>.

Due to the insertion of the instrument in the well, the flow is initially swirling and multidirectional. If the borescope is moved after being placed into the well, swirling flow will continue. Consequently, it is necessary to secure the instrument cable at the surface to prevent movement of the borescope. Generally, after 20-30 min, laminar horizontal flow dominates and has been observed in wells for periods of up to 48 h. Horizontal flow is observed at numerous locations based on particles that remain in the instrument's focal plane of 0.1 mm during transport

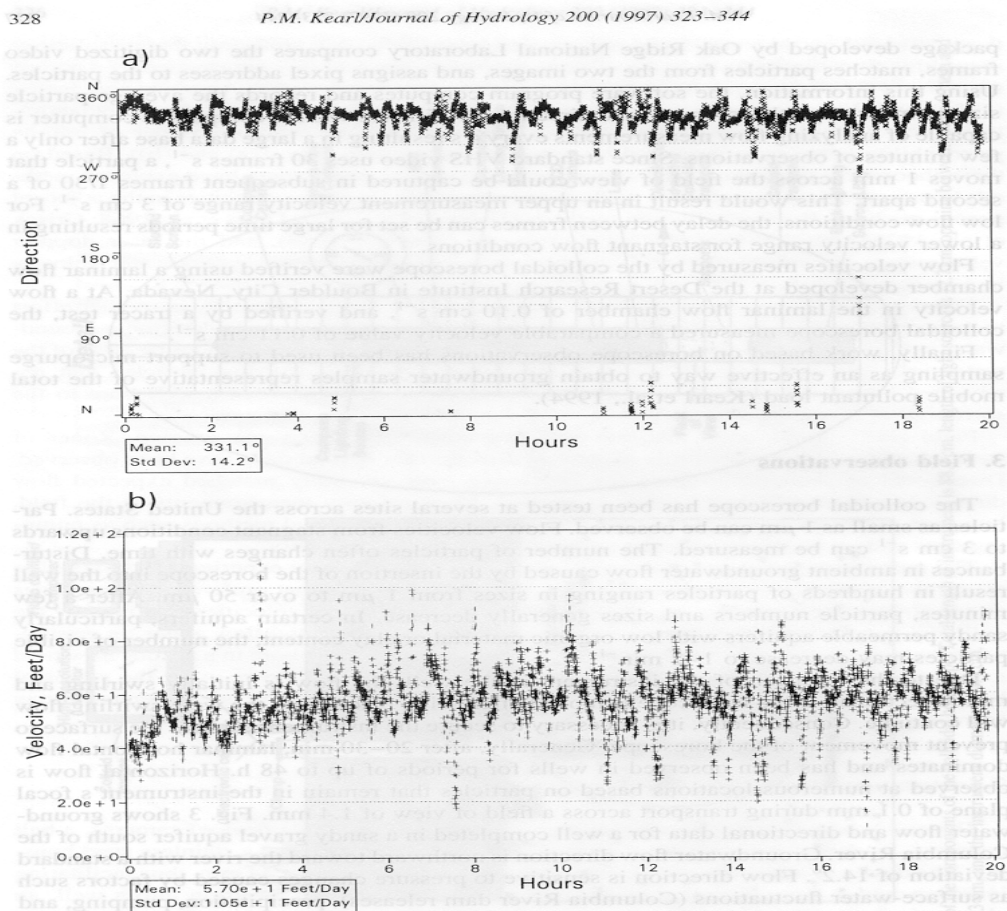


Fig. 3. Results of colloidal borescope flow observations in a monitoring well located south of the Columbia River showing (a) groundwater flow directions toward the river, (b) groundwater flow rates.

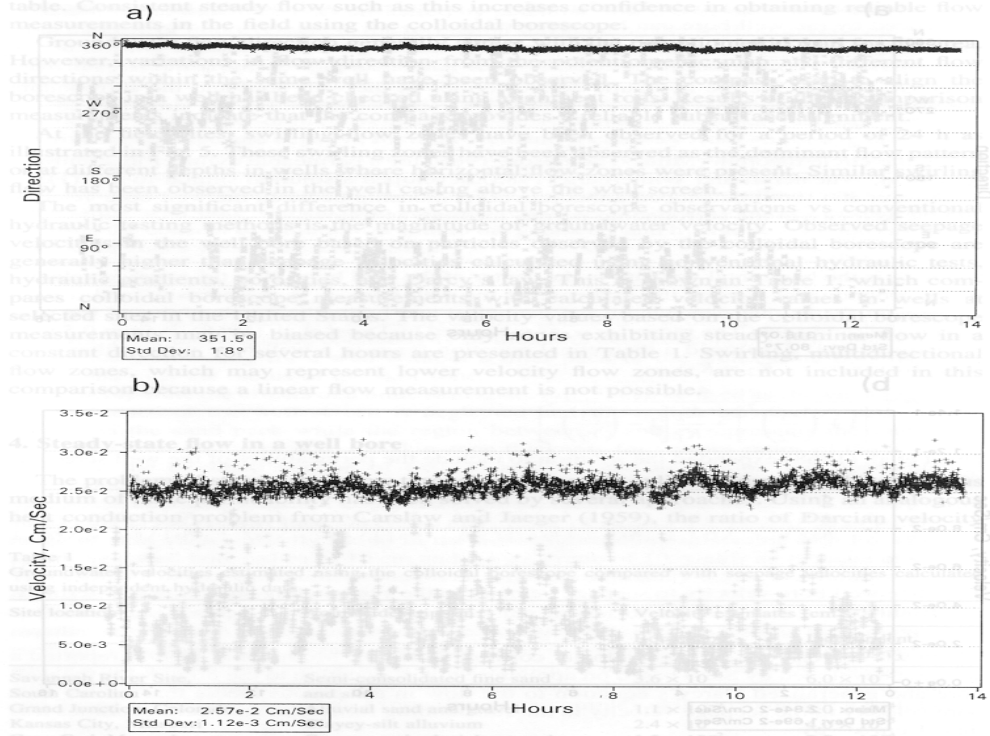


Fig. 4. Results of colloidal borescope flow observation near Paducah, Kentucky, showing (a) uniform flow direction toward drainage ditch, (b) groundwater flow rates.

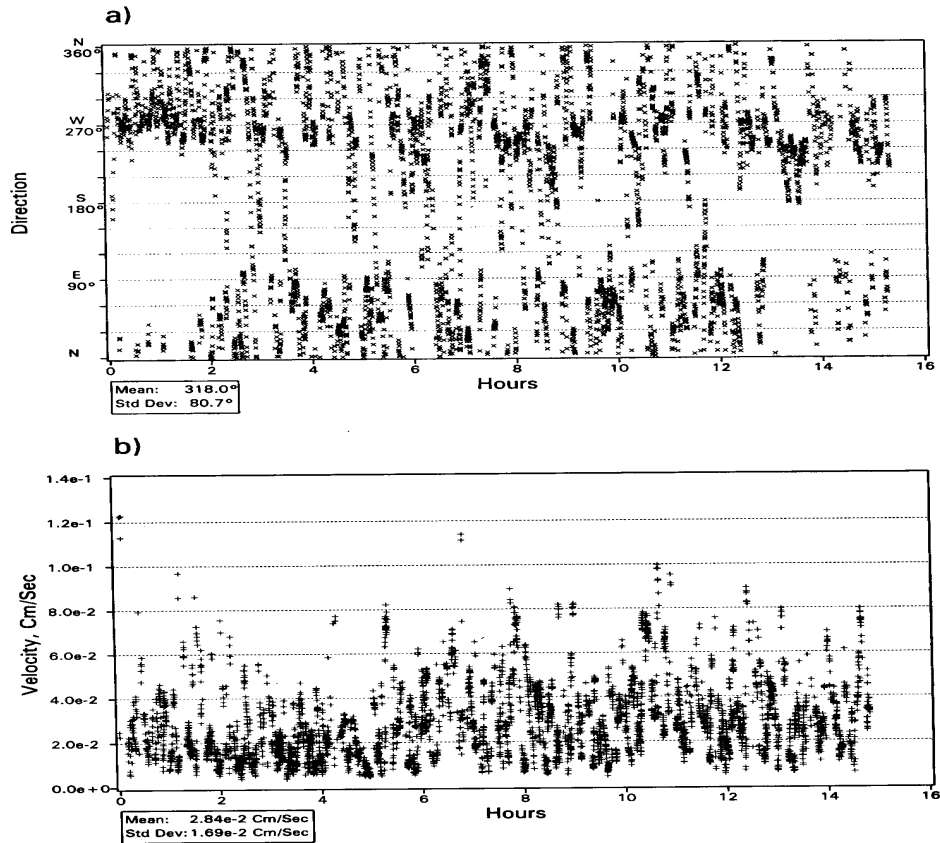


Fig. 5. Results of colloidal borescope flow observations near Livermore, California, showing (a) swirling flow conditions, (b) associated groundwater flow rates.

across a field of view of 1.4 mm. Fig. 3 shows ground- water flow and directional data for a well completed in a sandy gravel aquifer south of the Columbia River. Groundwater flow direction is northward toward the river with a standard deviation of 14.2'. Flow direction is sensitive to pressure changes caused by factors such as surface-water fluctuations (Columbia River dam releases), precipitation, pumping, and nearby heavy traffic. For example, the colloidal borescope instantaneously observes a pressure wave generated by dropping a bailer into a well at a distance of 10 m.

Fig. 4 shows groundwater flow and directional data for a well near a field site in Kentucky. Steady flow directions and velocities were observed for over 17 h in this well. The flow direction is directly toward a drainage ditch that intersects the water table. Consistent steady flow such as this increases confidence in obtaining reliable flow measurements in the field using the colloidal borescope.

Groundwater flow direction generally agrees with the potentiometric map for the area. However, variations in flow direction from the potentiometric map and different flow directions within the same well have been observed. The compass used to align the borescope in a well has been checked using alignment rods. Results of these comparison measurements indicate that the compass provides a reliable subsurface alignment.

At the field sites, swirling flow zones have been observed for a period of 24 h as illustrated in Fig. 5. These swirling zones have been observed as the dominant flow pattern or at different depths in wells where horizontal flow zones were present. Similar swirling flow has been observed in the well casing above the well screen.

The most significant difference in colloidal borescope observation vs. conventional hydraulic testing methods is the magnitude of groundwater velocity. Observed seepage velocities in the well bore based on particles observed by the colloidal borescope are generally higher than seepage velocities calculated using conventional hydraulic tests, hydraulic gradients, porosities, and Darcy's law. This is shown in Table 1, which compares colloidal borescope measurements with calculated velocity values in wells at selected sites in the United States. The velocity values based on the colloidal borescope measurements may be biased because only zones exhibiting steady laminar flow in a constant direction for several hours are presented in Table 1. Swirling, multidirectional flow zones, which may represent lower velocity flow zones, are not included in this comparison because a linear flow measurement is not possible.

### ***Steady-state flow in a well bore***

The problem of steady-state flow through a permeable cylinder surrounded by a porous medium of finite permeability has been solved by several approaches. Using an analogous heat conduction

problem from Carslaw and Jaeger (1959), the ratio of Darcian velocity

**Table 1**

Groundwater velocities estimated using the colloidal borescope compared with seepage velocities calculated using independent hydraulic data

| Site location           | Aquifer description                  | Velocity             |                      |
|-------------------------|--------------------------------------|----------------------|----------------------|
|                         |                                      | Borescope            | Independent          |
| Savannah River Site, SC | Semi-consolidated fine sand and silt | $3.6 \times 10^{-3}$ | $6.0 \times 10^{-5}$ |
| Grand Junction, CO      | Alluvial sand and gravel             | $1.1 \times 10^{-2}$ | $8.0 \times 10^{-4}$ |
| Kansas City, MI         | Clayey silt alluvium                 | $2.4 \times 10^{-3}$ | $4.0 \times 10^{-5}$ |
| Cape Cod, MA            | Coarse sand, glacial outwash         | $1.2 \times 10^{-2}$ | $7.7 \times 10^{-4}$ |
| Paducah, KY             | Alluvial sands and gravels           | $1.0 \times 10^{-2}$ | $8.0 \times 10^{-4}$ |

inside the well bore ( $q_0$ ) to the Darcian velocity outside the well bore ( $q_3$ ) at a distance not influenced by the well bore can be expressed as

$$\frac{\rho_0}{\rho_3} = \frac{2(K_0 / K_3)}{1 + (K_0 / K_3)} \quad (1)$$

where  $K_0$  and  $K_3$  are the hydraulic conductivities in the well bore and the surrounding porous medium, respectively. As the ratio  $K_0/K_3$  approaches  $\infty$ , Eq. (1) simplifies to

$$q_3 = \frac{q_0}{2} \quad (2)$$

Using the circle theorem (Milne-Thompson, 1968) for a permeable cylinder in a uniform flow field, Wheatcraft and Winterberg (1985) developed a solution similar to Eq. (1).

Drost et al. (1968) developed a theoretical relationship between the well bore velocity and the velocity in the surrounding porous medium as follows

$$\bar{v}_3 = \frac{\bar{v}_0}{\alpha n_3} \quad (3)$$

where  $\bar{v}_0$  is the horizontal velocity in the center of the well bore,  $\bar{v}_3$  is the seepage velocity of the groundwater beyond the influence of the well bore,  $n_3$  is the porosity, and  $\alpha$  is an adjustment factor that depends on the geometry and hydraulic conductivity of the well screen and sand pack.

The range for  $\alpha$ , as measured by Drost et al. (1968), is from 0.5 to 4.

Ogilvi (1958) developed a theoretical equation for  $\alpha$  in a Well bore with a filter pack

(Fig. 1 (c):  $r_2 = r_3$ ,  $K_2 = K_3$ )

$$\alpha = \frac{4}{\left[1 + \left(\frac{r_1}{r_2}\right)^2\right] + \frac{K_2}{K_1} \left[1 - \left(\frac{r_1}{r_2}\right)^2\right]} \quad (4)$$

Drost et al. (1968) expanded the solution to include the permeability of the well screen as described by

$$\alpha = \frac{8}{\left(1 - \frac{K_3}{K_2}\right) \left[1 + \left(\frac{r_1}{r_2}\right)^2\right] + \frac{K_2}{K_1} \left[1 - \left(\frac{r_1}{r_2}\right)^2\right] + \left(1 - \frac{K_3}{K_2}\right) \left[\left(\frac{r_1}{r_3}\right)^2 + \left(\frac{r_1}{r_3}\right)^2\right] + \frac{K_2}{K_1} \left[\left(\frac{r_1}{r_3}\right)^2 - \left(\frac{r_2}{r_3}\right)^2\right]} \quad (5)$$

To relate well bore velocity to seepage velocity in the surrounding aquifer, a new term,  $\bar{\alpha}$ , is introduced:

$$\bar{\alpha} = n_3 \alpha \quad (6)$$

which we will call the seepage velocity conversion factor. Momii et al. (1993) Reported a solution developed by Sano based on applying Stokes' equation to the flow inside the well bore and generalized Darcy's equation to the flow in the porous media that relates well bore velocity to the seepage velocity in the surrounding formation with permeabilities less than  $1 \text{ cm s}^{-1}$  by

$$\bar{v}_3 = \frac{v_0}{\bar{\alpha}} \quad (7)$$

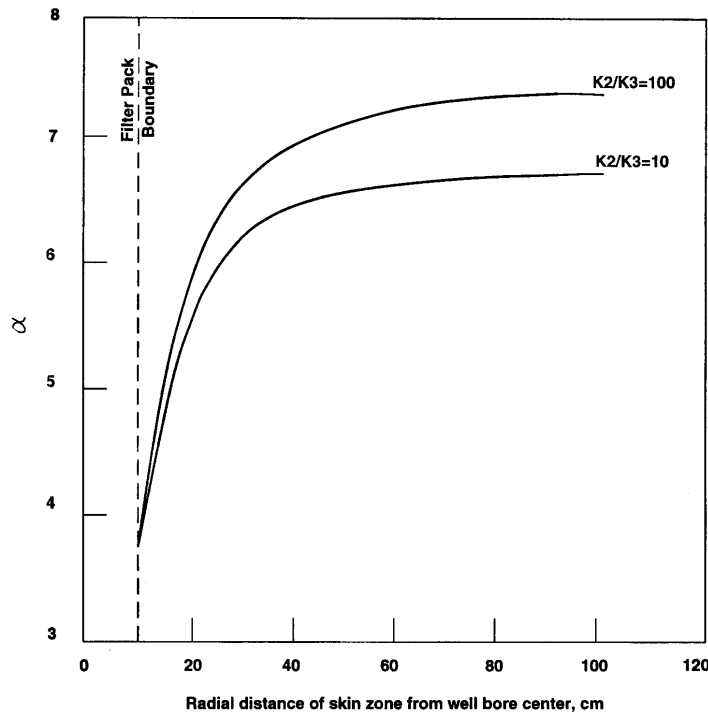


Fig. 6. Impact of skin thickness on flow in a well bore for different ratios of skin to formation hydraulic conductivity.

where  $\bar{\alpha}$  equals 3 according to Sano's theory. Using a laser doppler velocimeter, Momii et al. (1993) verified Sano's theory in the laboratory.

Skin effects, which are not considered by potential flow theory or Sano's theory, result from damage or improvement to the formation surrounding the well bore. Damage may be due to drilling fluids or smearing of fine-grain material on the well bore walls. Improvement may result from development that removes fine-grain material and increases the permeability of the formation adjacent to the well bore.

Earlougher (1977) presented the concept of a finite well skin surrounding the well bore. The degree of damage (or improvement) is expressed in terms of a skin factor ( $s$ ), which is positive for damage and negative for improvement. It can vary from -5 for a hydraulically fractured well to +- for a well that is too badly damaged to produce (Earlougher, 1977). Positive skin effects result in a flow velocity decrease and may be responsible for swirling flow zones observed in some wells. Therefore, only negative skin effects are considered for relating well bore velocities to seepage velocities in the surrounding porous media. Relating the concept of a finite well skin to the geometry and hydraulic conductivity of the individual zones yields the relationship

$$s = \left( \frac{K_3}{K_2} - 1 \right) \ln \left( \frac{r_3}{r_2} \right) \quad (8)$$

where  $s$  is a skin factor,  $K_3$  is the hydraulic conductivity of the surrounding porous medium,  $K_2$  is the hydraulic conductivity of the finite skin zone,  $r_2$  is the well bore radius (either the well casing for a well without a filter pack or the well casing plus the filter pack), and  $r_3$  is the radius of the skin zone.

To incorporate the effects of a finite skin zone, Eq. (5) can be used as shown in Fig. I (d). The influence of the well screen is neglected and the region between  $r_1$  and  $r_2$  now represents the sand pack while the region between  $r_2$  and  $r_3$  represents the finite skin zone. The relationship of  $a$  to the skin zone thickness for various ratios of the  $K_2$  to  $K_3$  based on the modified version of Eq. (5) is illustrated in Fig. 6. It is apparent that significant increases in  $a$  occur with an increase in permeability in a concentric ring of only a few centimeters in thickness. To estimate the radius of a finite skin zone, Bidaux and Tsang (1991) report that a negative skin value of -2 is a reasonable value within the range of skin values usually found in the field. Substituting this value into Eq. (8), and assuming a well bore radius of 10 cm and a  $K_2/K_3$  ratio of 10, yields an  $r_3$  value of 92 cm. This estimate of the skin radius produces an  $a$  of approximately 6.5. A maximum value for  $a$  of 8 is possible based on Eq. (5).

Bidaux and Tsang (1991) suggested that the model of a finite skin consisting of an annular region with a constant hydraulic conductivity differing from the unperturbed medium is not realistic. Instead, the skin zone is a region that is radially nonuniform and reaches a maximum hydraulic conductivity close to the well bore, decreasing gradually to the formational hydraulic

conductivity at some distance from the well bore. Bidaux and Tsang (1991) developed an expression for a complex skin surrounding a well bore:

$$\frac{K(r)}{K_3} = \exp\left(-\frac{u}{(r/r_2)}\right) \quad (9)$$

The term  $u$  is the magnitude of the permeability changes close to the well. Similar to the skin factor  $s$  in Eq. (8), a positive value of  $u$  means a permeability decrease near the well (damage) and a negative value indicates that the well is developed. The parameter  $\gamma$  can be interpreted in terms of thickness of the damage or developed zone: the lower the value of the thicker the skin.

Based on the concept of a complex skin, Bidaux and Tsang (1991) introduced the convergence factor  $\Xi$  to relate apparent Darcy velocity in the well (resulting from the deformation of streamlines due to an infinitely conducting well and the presence of a complex skin) to the Darcy velocity in the undisturbed formation:

$$q_0 = \frac{q_3}{\Xi} \quad (10)$$

For a constant potential well bore boundary without skin effects,  $\Xi$  equals 2, which agrees with Eq. (2). However, the complex skin model can yield, for reasonable values of  $s$ , convergence factors that equal or exceed 10.

Based on the literature review of theoretical models for groundwater flow in a well bore, a range of seepage velocity conversion factors of less than 1 upwards to 4 are possible for a range of effective porosities from 0.1 to 0.5. Theoretical development for flow in a homogeneous isotropic media developed by Sano's theory yielded a seepage velocity conversion factor of '3. Considering the effects of varying permeability resulting from well screens and sand packs, Drost et al. (1968) experimentally determined a seepage velocity conversion factor for the specified porosity range of less than 1 upwards to 2. Work presented in this paper that modifies Drost's work to include the Bidaux and Tsang (1991) model that the skin zone permeability is radially nonuniform and reaches a maximum hydraulic conductivity close to the well bore yields a seepage velocity conversion that ranges up to 4. The complex skin model presented by Bidaux and Tsang (1991) suggests the range may be higher.

Finally, well screen influences on flow rates and direction in a well bore have been studied by Drost et al. (1968) and Kerfoot and Massard (1985). Using a tracer experiment, Drost et al. (1968) demonstrated that flow directions in a well bore are consistent with flow directions in the surrounding porous medium (Fig. 1(a) and (b)). Kerfoot and Massard (1985) show that increasing the frequency of slots in the well screen and the number of slot rows allows accuracies of direction measurements of  $\pm 4^\circ$ .

## Laboratory experiment

The laboratory experiments were designed to evaluate the effects of well size, degree of well screen penetration, filter pack, and aquifer heterogeneity under controlled flow conditions. A

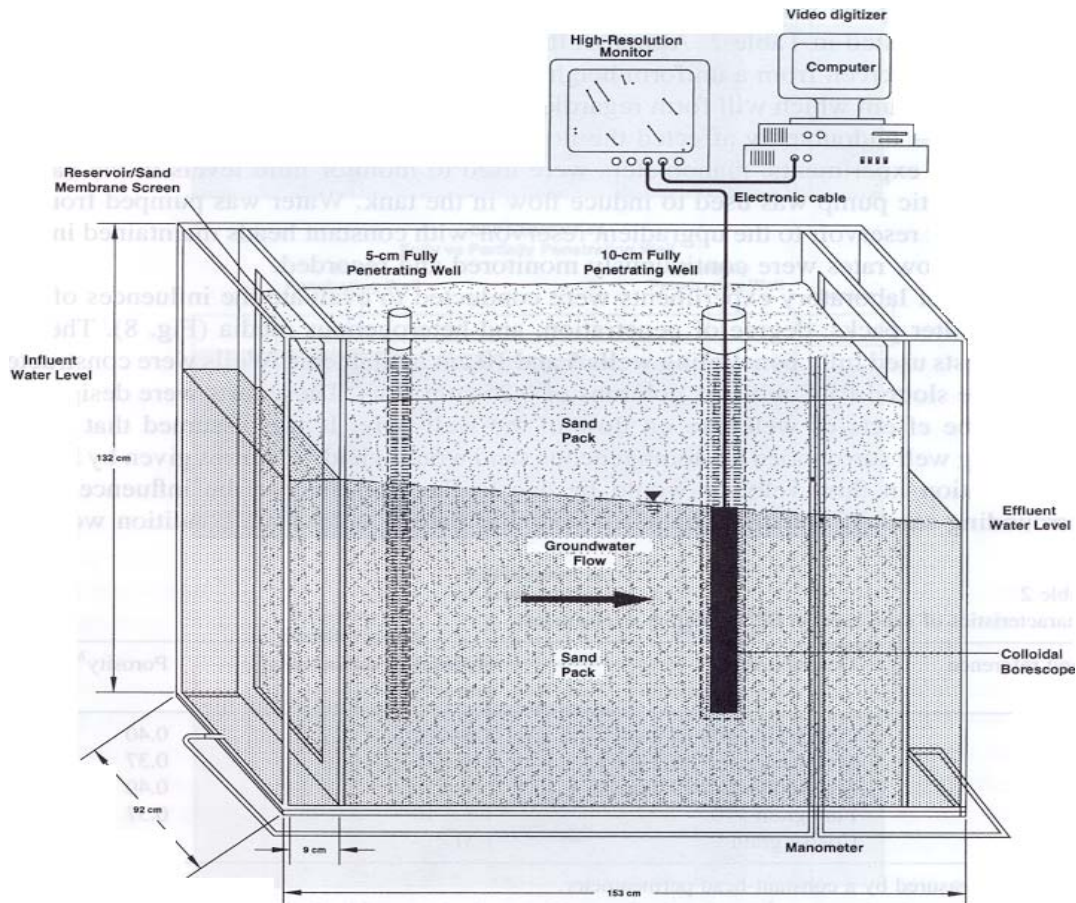


Fig. 7. Sand tank used for the laboratory experiments.

sand tank measuring 153 cm in length, 92 cm in width, and 132 cm in height was built with two screened baffles separating the sand from the reservoirs at both ends of the tank (Fig. 7). The reservoirs were connected to manometers for measuring fluid heads.

Prior to placing the sand into the tank, the sides and bottom were coated with paraffin wax. After sand placement, the sides and bottom were heated, allowing the wax to partially flow into the sand. The purpose of the wax was to prevent preferential flow channels from developing along the sides and base of the tank. Sand descriptions and hydraulic conductivities are listed in Table 2. Although the tank was packed by carefully dropping the sand through a screen from a uniform height, small-scale heterogeneities were created in the porous medium, which will form regardless of how carefully the sand is placed. These heterogeneities undoubtedly affected the flow characteristics in the sand tanks.

During the experiments, manometers were used to monitor fluid levels in the baffles, and a peristaltic pump was used to induce flow in the tank. Water was pumped from the downgradient

reservoir to the upgradient reservoir with constant heads maintained in both reservoirs. Flow rates were continuously monitored and recorded.

Four sets of laboratory experiments were conducted to evaluate the influences of well diameter, filter packs, degree of penetration, and heterogenous media (Fig. 8). The first series of tests used fully penetrating wells 5 and 10 cm in diameter. Wells were constructed of machine slotted PVC with six columns of 0.25-mm slots. These tests were designed to evaluate the effects of well size on flow in the well bore. It was assumed that a fully penetrating well surrounded by homogeneous sand would yield velocities given by Eq. (3). Any variation in flow velocity would be due to the well size or the influence of the surrounding sand. If velocities matched potential theory, a baseline condition would be established where other potential sources of variation such as filter packs, partially penetrating wells, or aquifer heterogeneity could be evaluated.

Table 2

Characteristics of sand used in the laboratory experiments

| Sand Reference No. | Description                          | Hydraulic conductivity <sup>a</sup> (cm s <sup>-1</sup> ) | Porosity <sup>b</sup> |
|--------------------|--------------------------------------|---|-----------------------|
| 1                  | Fine-grain bedding sand              | $2.5 \times 10^{-3}$                                      | 0.40                  |
| 2                  | Medium grain #30 type 1 <sup>c</sup> | $1.3 \times 10^{-1}$                                      | 0.37                  |
| 3                  | Medium grain #30 type 2              | $6.4 \times 10^{-2}$                                      | 0.40                  |
| 4                  | Fine grain #70                       | $1.8 \times 10^{-2}$                                      | 0.37                  |
| 5                  | Coarse grain                         | 1.31  | 0.38                  |

a Values measured by a constant-head permeameter.

b Porosity determined on samples using similar packing method as used in the large sand tank

c Refers to supplier.

The second series of tests used two fully penetrating, 5-cm-diameter wells. One of the wells was surrounded by a 12.5-cm-diameter coarse-grain filter pack. The purpose of this design was to evaluate filter-pack effects on the flow velocities in the sand tank according to theory discussed by Drost et al. (1968). The sand pack was constructed by placing a 12.5-cm-diameter thin-wall aluminum tube around the well. The tank was filled sand and the annular space between the well and aluminum tube filled with coarse-grain sand. The aluminum tube was then removed resulting

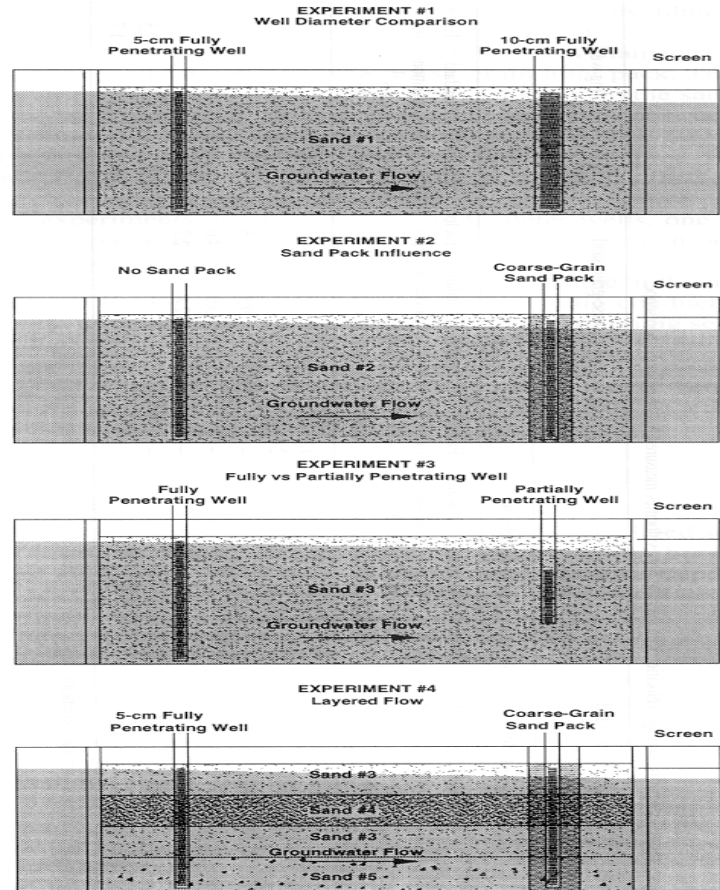


Fig. 8. Experimental setups to assess flow variations under different conditions.

in a uniform sand pack surrounding the well.

The third set of experiments involved two 5-cm-diameter wells, one fully penetrating and the other partially penetrating. This design allowed for an evaluation of vertical flow convergence to a partially penetrating well.

The final set of experiments was designed to evaluate the influence on well bore velocities of a layered porous medium with varying hydraulic conductivities. The sand tank was packed with three different types of sand in an upward fining sequence typical of field situations. A layer of medium-grain sand was placed on top to allow saturation of the fine-grain sand layer. Two fully screened wells, one with a filter pack using the same coarse-grain sand that comprised the basal layer and one without, were installed in the sand tank. Directions and flow rates were measured at several locations within each individual layer.

Table 3  
Laboratory results comparing seepage velocities with average flow velocities measured by the colloidal borescope

| Calculated <sup>a</sup><br>seepage velocity<br>( $\text{cm s}^{-1} \times 10^{-3}$ ) | Homogeneous sand  |  |                              | Well with coarse-grain sand<br>pack                           |  |                              | Partially penetrating well                                    |  |                              |
|--|---|--|------------------------------|---|--|------------------------------|---|--|------------------------------|
|  | Measured<br>velocity<br>( $\text{cm s}^{-1} \times 10^{-3}$ ) | Standard<br>deviation<br>( $\text{cm s}^{-1} \times 10^{-3}$ ) | Factor<br>( $\bar{\alpha}$ ) | Measured<br>velocity<br>( $\text{cm s}^{-1} \times 10^{-3}$ ) | Standard<br>deviation<br>( $\text{cm s}^{-1} \times 10^{-3}$ ) | Factor<br>( $\bar{\alpha}$ ) | Measured<br>velocity<br>( $\text{cm s}^{-1} \times 10^{-3}$ ) | Standard<br>deviation<br>( $\text{cm s}^{-1} \times 10^{-3}$ ) | Factor<br>( $\bar{\alpha}$ ) |
|  | 5-cm-diameter base-line wells                                 |  |                              |   |  |                              |   |  |                              |
|  | 10-cm-diameter well   |  |                              |   |  |                              |   |  |                              |
| 1.1  | 2.8   | 1.1  | 2.5                          | 2.0   | 1.2  | 1.8                          | -   | -  | -                            |
| 2.4  | 5.9   | 1.5  | 2.5                          | 6.2   | 2.8  | 2.6                          | -   | -  | -                            |
| 7.5  | 7.4   | 4.7  | 1.0                          | -   | -  | -                            | 26.5  | 9.5  | 3.5                          |
| 15.0   | 30.0  | 14.3   | 2.0                          | -   | -  | -                            | 59.7  | 13.0   | 4.0                          |
| 22.3   | 47.7  | 11.8   | 2.1                          | -   | -  | -                            | 60.2  | 12.8   | 2.7                          |
| 9.4  | 23.6  | 20.6   | 2.5                          | -   | -  | -                            | -   | -  | -                            |
| 12.0   | 19.3  | 10.6   | 1.6                          | -   | -  | -                            | -   | -  | -                            |
|  |   |  |                              |   |  |                              | 24.0  | 6.3  | 2.5                          |
|  |   |  |                              |   |  |                              | 20.5  | 12.3   | 1.7                          |

<sup>a</sup> Determined from hydraulic measurements.

## Results

Table 3 is a summary of the laboratory results comparing calculated seepage velocities with average flow velocities in the wells as measured by the colloidal borescope. Well bore velocities represent an average of 15 measurements at incremental depths in the wells.

Seepage velocities for the surrounding porous medium were calculated using flow rates from the recirculation pump, measured porosities, and the cross-sectional area of the tank. For the four laboratory tests comparing well diameters, filter packs, partially penetrating wells, and heterogeneity, a fully penetrating 5-cm-diameter well without a filter pack was used as a baseline. In the laboratory tests, flow directions in test wells measured by the colloidal borescope were consistent with flow directions in the sand tank. Directional variations as a function of depth for the individual well tests yielded an average standard deviation of 7'. The notable exception occurred in the low permeable zones of the layered sand tank tests. Swirling multidirectional flows, similar to field conditions, were observed in these zones.

Comparing seepage velocities with colloidal borescope measurements for the baseline wells shows a factor (a) of 1.0 to 2.5 times higher than calculated seepage velocities, with an average a of 2.0 for the baseline wells. Boreoscope measurements showed that there could be variations in groundwater flow in a well as a function of depth. This variation is believed to be the result of heterogeneities in the adjacent porous medium. Regardless of how carefully the packing was done in the large tank, it was impossible to obtain a completely homogenous porous medium. This observation is consistent with those of homogenous sand packs (Ripple et al., 1974).

Laboratory results for fully penetrating wells with and without filter packs compared favorably with the prediction of Drost et al. (1968). For the well that was not surrounded by a coarse-grain filter pack, velocities were approximately one half of the values for the well surrounded with a filter pack. Flow velocities in the filter-pack well ranged from 2.7 to 4.0 times higher than the calculated seepage velocities. It is clear that the filter pack allows a significant increase in flow velocities in the well.

Results from the third laboratory test indicated no significant difference between the average seepage velocities in the fully penetrating and the partially penetrating well *P.M. Kearl* (Journal (Table 3)). These results indicate that vertical flow convergence is not a major factor affecting velocity in a well. Possible explanations include the cap at the base of the well that restricts

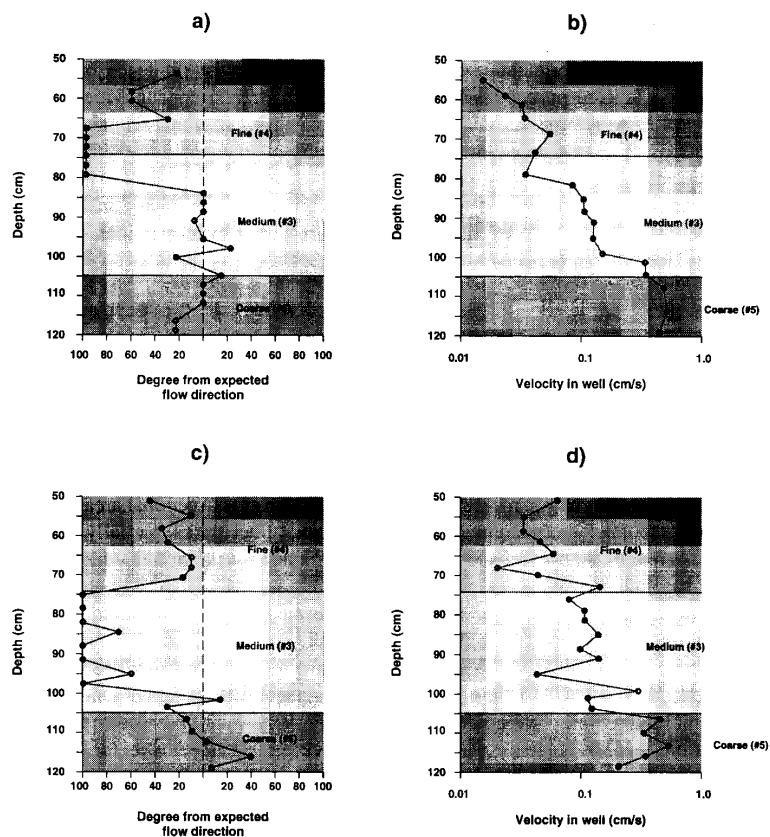


Fig. 9. Results of groundwater velocity measurements for the layered filter flow rates for (a) flow directions for filter-packed well; (b) flow rates for packed well; (c) flow direction for well without a filter pack; (d) flow rates for well without a filter pack.

vertical flow or lower vertical hydraulic conductivity in the sand tank that restricts vertical flow. For aquifers where natural vertical flow components are minor, these results suggest that vertical flow convergence from an unscreened or uncased portion of the aquifer is not a major factor affecting velocity in a well.

The layered sand tank measurement results are illustrated in Fig. 9. Variations in direction and flow rate between successive measurements were significantly less in the well with a filter pack than in the well without a filter pack. Moreover, the higher the velocity, the lower the variation in flow. This was the case for filter pack wells, which exhibited higher velocities than wells without a filter pack, and is consistent with decreasing coefficients of variation with increases in the velocity that was observed in most of the earlier tests.

Velocity measurements in the basal coarse-grain sand yielded a seepage velocity conversion factor of approximately 2, similar to the baseline well measurements. Minor directional variations in flow were similar to the field test shown in Fig. 4. Significant variations in both flow direction and velocities, however, were observed in the medium- and fine-grain units. For the filter pack well, direction in the medium-grain zone near the contact with the coarse-grain sand was consistent with expectations but varied dramatically near the contact with the fine-grain sand layer. Swirling flow, similar to field observations, characterized the flow near the upper contact. Large variations in flow directions, similar to Fig. 5, were typical for the upper medium and fine grain zones. In addition, well bore velocities for both the medium-grain and fine-grain sands were approximately five times greater than well bore velocities for the same sands measured in homogenous conditions under the same hydraulic gradient. Similar to a stream channel and side eddies, the momentum from high flow velocities in the coarse-grain section of the well bore is being transferred to the lower flow zones adjacent to the medium- and fine-grain sand layers. This result in higher velocities, with swirling, multidirectional flow, in the well bore adjacent to these low-permeable zones.

This behavior in the laboratory could explain field observations. Distinct flow zones with uniform flow directions have been observed adjacent to swirling flow zones. This could be interpreted as preferential flow zones with adjacent low-permeable zones. If this is the case, then implications for field use would include locating zones where steady directional flow is present and assuming that these zones are the preferential flow zones for that particular screened interval. If the interpretations and assumptions are correct, the magnitude of the velocity in these preferential flow zones would be greater than that predicted by hydraulic techniques that are averaged over the entire screened interval.

### ***Discussion and conclusions***

The results of the laboratory measurements are in reasonable agreement with predicted results

from theoretical models presented in the literature. Laboratory measurements have shown a minimum seepage velocity conversion factor ( $\alpha$ ) of 1 and a maximum value of 4. Therefore, using  $\bar{\alpha}$  conversion factor of 1-4 provides an acceptable range for calculating seepage velocity in the adjacent porous medium from velocity measurements in most field monitoring wells.

Results of the colloidal borescope measurements in the layered sand tank tests provide an explanation of the behavior of fluids in wells observed in the field. In the coarse sand layer or preferential flow zone, steady laminar flow conditions in the expected direction and at velocities two times higher than the adjacent porous media were measured. Only minor variations in direction as a function of time, similar to Fig. 4, were observed in the coarse sand layer. Flow in the well adjacent to the fine sand layer was generally swirling flow at a velocity higher than predicted by theoretical models. In addition, a high degree of directional variability similar to Fig. 5 was observed in the medium- and fine-grain zones.

Fig. 10(a) shows laboratory tests of flow with separation in a highly divergent channel (Schlichting, 1987). An analogy for flow in a well under ambient conditions as impacted by a heterogeneous formation is illustrated in Fig. 10(b). For the flow in the divergent channel, a vortex results in the region adjacent to the main flow channel. This vortex is similar to the swirling flow observed by the colloidal borescope in low permeable zones, both in the laboratory and the field. Swirling flow has also been observed in the well casing above the well screen. The laboratory tests have shown that several factors including aquifer heterogeneity, filter packs, and well skins influence flow in a well bore. For the colloidal borescope to be an effective tool in characterizing groundwater flow velocity, it is necessary to differentiate and quantify these effects. This is a difficult task because the hydraulic conductivity of the filter pack and surrounding formation may be unknown and/or the skin effects not easily quantified. However, following some basic assumptions and general guidelines, it is possible to select reliable data and estimate a range of groundwater velocities.

First, only zones that display consistent horizontal laminar flow in a steady direction over a substantial time period (greater than 2 h) should be considered. Swirling flow zones may be the result of adjacent, low-permeable sediments, positive skin effects, vertical flow gradients, or nearby preferential flow zones that dominate flow in the observed zone. Measurements in swirling flow zones should be disregarded. However, if steady directional flow is typical of the flow zone, then reliable measurements are possible.

At field sites, observed well bore flow velocities exceed predicted velocities, even values that are adjusted based on values. If theoretical work and laboratory results indicate that the borescope provides reliable flow measurements within a specified range, then this evidence would suggest that velocities in the well bore represent the maximum flow velocities in an aquifer. It would

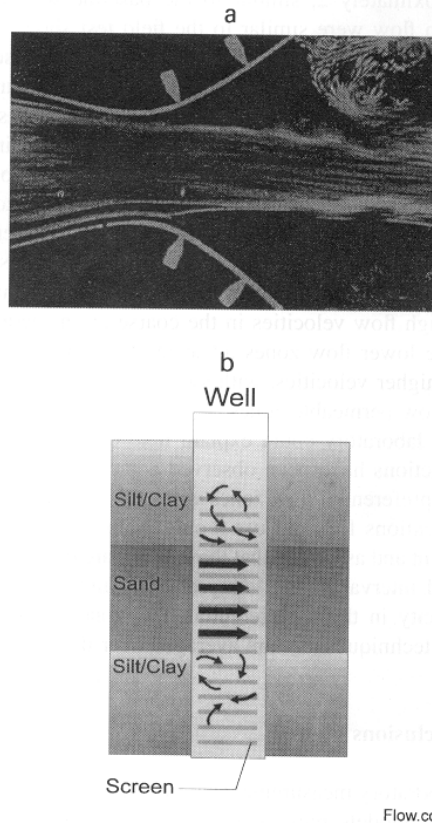


Fig. 10. (a) Flow with separation in a highly divergent channel (Schlichting, 1987), (b) analogous flow in a well bore resulting from a preferential flow zone.

further suggest that the maximum velocity and not the average linear velocity over the entire screen length dominate flow in the well bore under ambient flow conditions. In no instances have velocity measurements using the colloidal borescope been less than values predicted by independent hydraulic information. Swirling, nondirectional flow zones may be representative of lower-permeable material within the permeable section of the aquifer or positive skin effects due to poor well construction practices, but the flow velocity has been magnified by the transfer of momentum from adjacent, higher-flow zones.

Based on the work presented in this paper, colloidal borescope measurements in the field should be reduced by a factor of 1-4 to calculate seepage velocity in the adjacent porous medium. For field comparison measurements presented in Table 1, the borescope measurements represent the flow velocities in the preferential flow zones compared with average flow velocity measurement obtained by conventional methods. This statement is supported by laboratory observations in the layered sand tank experiments. Consequently, one could use these maximum velocity values measured by the colloidal borescope to estimate flow velocities in preferential flow zones in a heterogeneous aquifer.

In summary, the results of the laboratory experiments have shown that it is possible to quantify groundwater flow directions and rates under laboratory conditions by measuring particle velocities in a well bore using the colloidal borescope. Groundwater flow velocities measured by the

colloidal borescope in heterogeneous aquifers will be biased toward the maximum velocity values present in the aquifer. The colloidal borescope offers the interesting possibility of measuring the maximum seepage velocities present in a heterogeneous aquifer. If these velocity values were available, then a different approach to simulating mass transport would also become available. Models that incorporate the geometry of the flow system with assigned velocity vectors in the preferential flow zones could use molecular diffusion as an attenuating mechanism.

### ***Acknowledgements***

This work was conducted as part of the integrated demonstration program of the Department of Energy's Office of Technology Development.

The author wishes to thank Edward Kirk Roemer, Steve Sturm, and Scott List for their assistance with the laboratory and field measurements and Dr Clint Case for his review of the edited manuscript. In addition, reviewer comments helped clarify the theoretical and experimental results presented in this paper.

### ***References***

- Bidaux, P., Tsang, C.F., 1991. Fluid flow patterns around a well bore or an underground drift with complex skin effects, *Water Resource. Res* 27 (11), 2993-3008.
- Carslaw, H.S., Jaeger, J.C., 1959. *Conduction of Heat in Solids*. Oxford University Press, New York, 510 pp.
- Drost, W., Klotz, D., Koch, A., Moser, H., Neurnaier, F., Rauert, W., 1968. Point dilution methods of investigating ground water flow by means of radioisotopes. *Water Resour. Res.* 4 (1), 125-146.
- Earlougher, R.C., 1977. *Advances in Well Test Analysis*. Society of Petroleum Engineers of AIME, Dallas, TX.
- Grisak, G.E., Merritt, W.F., Williams, D.W., 1977. A fluoride borehole dilution apparatus for groundwater velocity measurements. *Can. Geotech J.* 14, 554-561.
- Halevy, E., Moser, H., Zellhofer, O., Zuber, A., 1967. Borehole dilution techniques: a critical review. In: *Isotopes in Hydrology*. IAEA, Vienna, pp. 531-564.
- Hess, A.E., 1986. Identifying hydraulically conductive fractures with a slow-velocity borehole flowmeter. *Can. Geotech. J.* 23, 69-78.

Kearl, P.M., Korte, N.E., Stites, M., Baker, J., 1994. Field comparison of micropurging vs traditional ground water sampling. *Ground Water Monit. Rev.* Fall, 183-190.

Kerfoot, W.B., 1988. Monitoring well construction and recommended procedures for direct ground-water flow measurements using a heat-pulsing flowmeter. In: Collins, A.G., Johnson, A.I. (Eds.), *Ground-Water Contamination: Field Methods*. American Society of Testing and Materials, Philadelphia, pp. 146-161.

Kerfoot, W.B., Massard, V.A., 1985. Monitoring well screen influences on direct flowmeter measurements. *Ground Water Monit. Rev.* Fall, 74-77.

Milne-Thompson, L.M., 1968. *Theoretical Hydrodynamics*. The McMillian Company, Inc., New York,

Molz, F.J., Morin, R.H., Hess, A.E., Melville, J.G., Guven, O., 1989. The impeller meter for measuring aquifer permeability variations: evaluation and comparison with other tests. *Water Resour. Res.* 25 (7), 1677-1683.

Molz, F.J., Boman, G.K., Young, S.C., Waldrop, W.R., 1994. Borehole flowmeters: field application and data analysis. *J. Hydrol.* 163, 347-371.

Momii, K., Jinno, K., Hirano, F., 1993. Laboratory studies on a new laser doppler velocirnetr system for horizontal groundwater velocity measurements in a borehole. *Water Resour. Res.* 29 (2), 283-291.

Ogilvi, N.A., 1958. An electrolytical method of determining the filtration velocity of underground waters. *Bull. Sci-Tech. Inf.* No. 4 (16), Gosgeoltekbisdat, Moscow (in Russian).

Ripple, C.D., James, R.V., Rubin, J., 1974. Packing-induced radial particle-size segregation: influence on hydrodynamic dispersion and water transfer measurements. *Soil Sci. Soc. Am.* 38, 219-222.

Schlchting, H., 1987. *Boundary-Layer Theory*. McGraw-Hill Book Co., New York, pp. 817.

Wheatcraft, S.W., Winterberg, F., 1985. Steady state flow passing through a cylinder of permeability different from the surrounding medium. *Water Resour. Res.* 21 (12), 1923-1929.